SUPPORTING INFORMATION

Optimization of the Pore Structure of Biomass-Based Carbons in Relation to Their Use for CO_2 Capture under Low- and High-Pressure Regimes

M. Sevilla,[a*] A. S. M. Al-Jumialy,[b] A. B. Fuertes,[a] R. Mokaya[b*]

[a] Instituto Nacional del Carbón (CSIC), Francisco Pintado Fe, 26, Oviedo 33011, Spain

[b] School of Chemistry, University of Nottingham, University Park, NG7 2RD Nottingham, UK.

[*] Corresponding authors: martasev@incar.csic.es (M. Sevilla); r.mokaya@nottingham.ac.uk (R. Mokaya)

Table S1. Physico-chemical properties of porous carbons obtained by chemical activation with potassium oxalate or potassium oxalate+melamine.

Carbon precursor	Code	Yield (%)	Textural properties			Chemical composition [wt %]		
			S_{BET} [m^2 g^{-1}]	V_p [cm^3 g^{-1}][a]	V_{micro} [cm^3 g^{-1}][b]	C	O	N
Sucrose	S-850	29	1470	0.59	0.57 (97)	-	-	-
Starch	A-850	18	1470	0.64	0.62 (97)	-	-	-
Sawdust	SW-800	25	1270	0.52	0.50 (96)	-	-	-
HTC glucose	HC-850	45	1600	0.69	0.61 (88)	-	-	-
Cellulose	C-3.6-1	4	3240	3.00	0.82 (27)	92.2	5.4	1.4
Sawdust	SW-3.6-2	15	3092	1.75	1.15 (66)	94.5	4.2	0.8

[a] Total pore volume was determined at a P/P_o of ~ 0.95. [b] Micropore volume was determined by using the Dubinin-Radushkevich equation or the QSDFT PSD. The percentage of pore volume that corresponds to micropores is indicated in parenthesis.

Table S2. CO_2 uptake at low pressure for top-performing carbon materials reported in the literature.

Material	CO_2 uptake @ 1 bar, 25 ºC [a] (mmol g^{-1})	Reference
G-800	4.5 (1.4)	This work
CS-6-CD-4	4.55 (1.1)	1
C-K-5	4.7 (1.5)	2
AS-2-600	4.8 (1.2)	3
NMC-600	3.9 (1.7)	4
SU-MAC-600/SU-MAC-500	4.2/4.5 (1.1/1.7)	5
600-2	4.8 (1.4)	6
ACGR2600/ACGR2700	4.3/4.9 (1.5)	7
ACCA2600/ACCA2700	4.7/5.0 (1.5)	7
SD2650P/SD2600P	5.3/5.8 (1.5/2.0)	8
MPPY2600	5.5 (2.1)	9
BIDC-0.5-700/BIDC-1-700	4.8/5.5 (1.8/2.0)	10
NAC-1.5-600	5.4 (~ 3)	11
CPC-550	5.8 (2.1)	12
C@MF-700	4.3 (1.8)	13

[a] CO_2 uptake at 0.15 bar is indicated in parenthesis.

Table S3. Chemical composition and textural properties of porous carbons obtained from glucose by chemical activation with a mixture of potassium oxalate and melamine at various activation temperatures (ratio glucose/potassium oxalate/melamine = 1 / 3.6 / 2).

T (ºC)	Yield (%)	Textural properties			Chemical composition [wt.%]			
		S_{BET} [m^2 g^{-1}]	V_p [cm^3 g^{-1}][a]	V_{micro} [cm^3 g^{-1}][b]	H	N	C	O
500	52	890	0.39	0.33 (85)	2.7	13.3	64.0	19.9
650	28	1522	0.69	0.59 (86)	2.1	9.8	70.8	17.3
750	9	3475	2.43	1.06 (44)	0.5	4.0	88.4	7.1
800	8	3460	2.72	1.00 (37)	0.5	2.7	92.4	4.4

[a] Total pore volume at P/Po ~ 0.95. [b] Micropore volume determined from the QSDFT PSD; the percentage of the total pore volume which corresponds to micropores is indicated in parenthesis.

Table S4. CO_2 uptake and working capacity at high pressure for top-performing carbon materials reported in the literature.

Material	CO_2 uptake @ 30 bar, 25 ºC [a] (mmol g^{-1})	Working capacity (PSA system)[d] (mmol g^{-1})	Reference
G-3.6-2	32.6 (49.1)	31.1	This work
AS-2M (hydrochar-derived KOH-AC)	26.1 (30.6)[b]	23.9	14
VR5-4:1 (mesophase pitch-derived KOH-AC)	27.6 (31.5)[c]	25	15
HPC5b2-1100 (hierarchical porous carbons)	27.4	23.7	16
PAF-1 (porous aromatic framework)	27.3 (30)[b]	25.3	17
SU-AC-400 (PANI-derived KOH-AC)	28.3 (35)	24	18
uGil-900 (asphalt-derived KOH-AC)	26.6 (35)	24	19
BIDC-3-700 (benzimidazole-derived KOH-AC)	28.1 (~33)[b]	~25	10
MPPY-4800 (polypyrrole-derived KOH-AC)	37.2 (54.1)	34.4	20

[a] Values in parenthesis correspond to a pressure of 50 bar. [b] CO_2 uptake at 40 bar. [c] CO_2 uptake at 45 bar. [d] Defined as the difference of equilibrium adsorption capacity at 30 and ~1 bar.

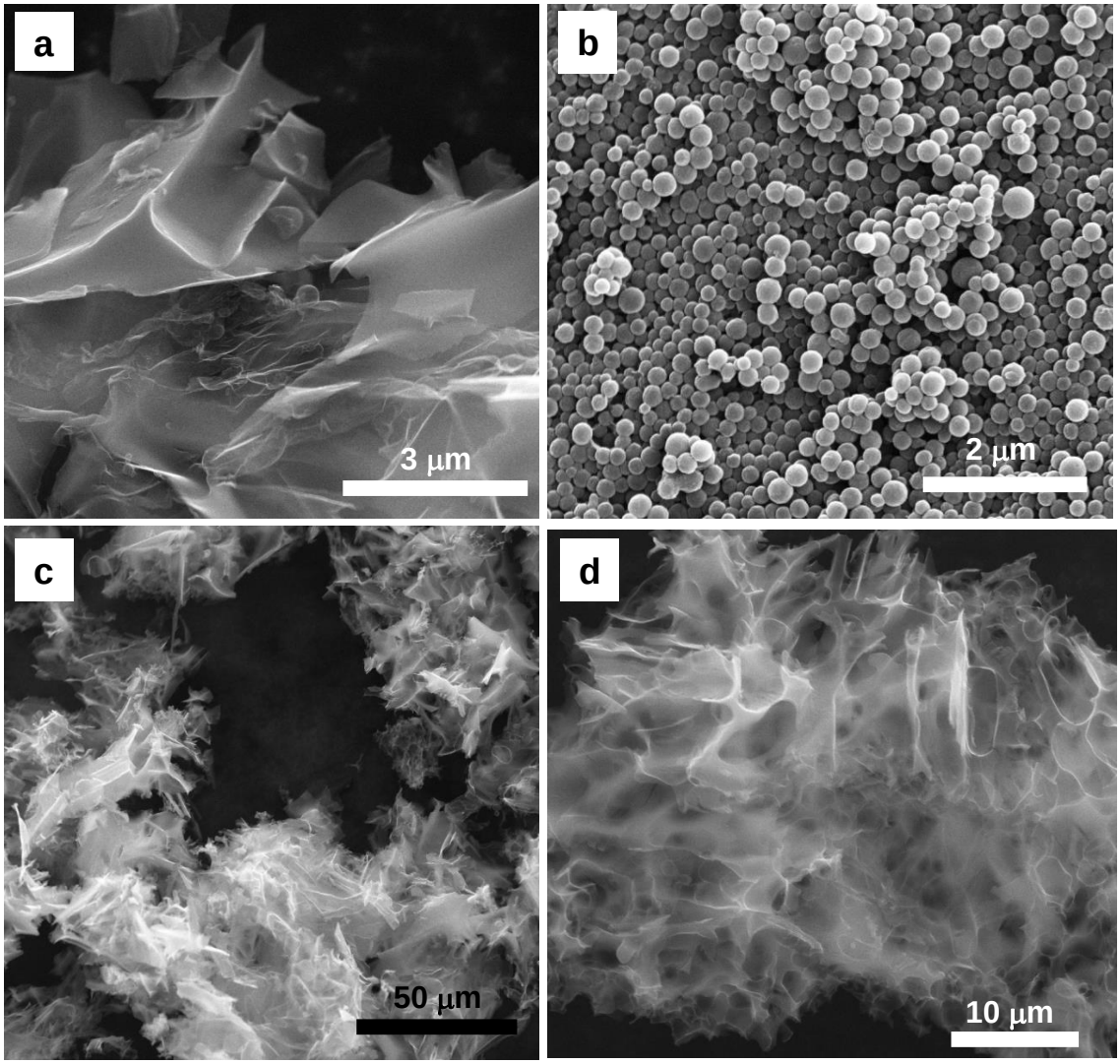

Figure S1. SEM images of the porous carbons obtained by chemical activation with potassium oxalate (activation temperature = 850 ºC) of a) glucose, b) glucose-derived hydrochar, c) and d) sucrose.

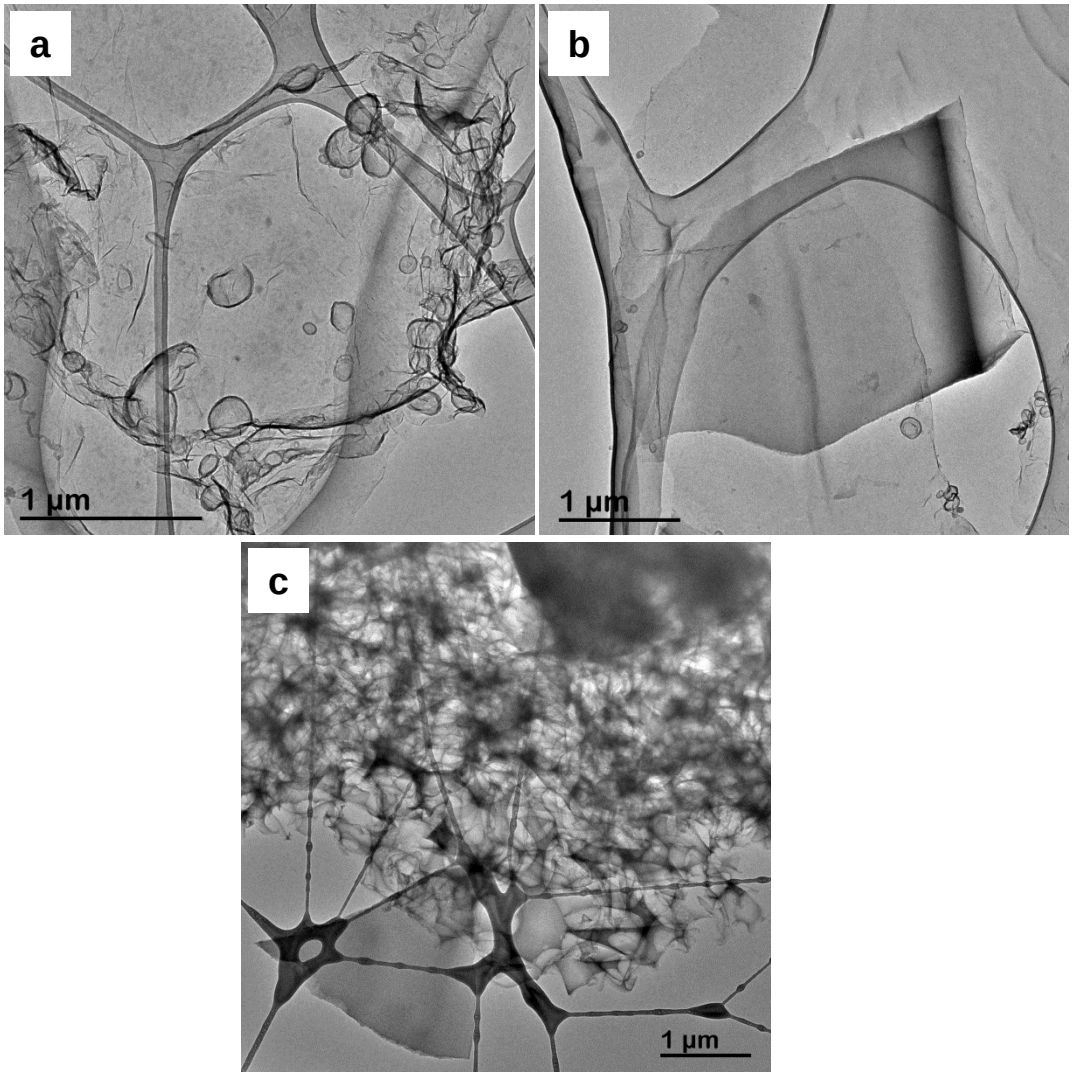

Figure S2. TEM pictures of sample G-850.

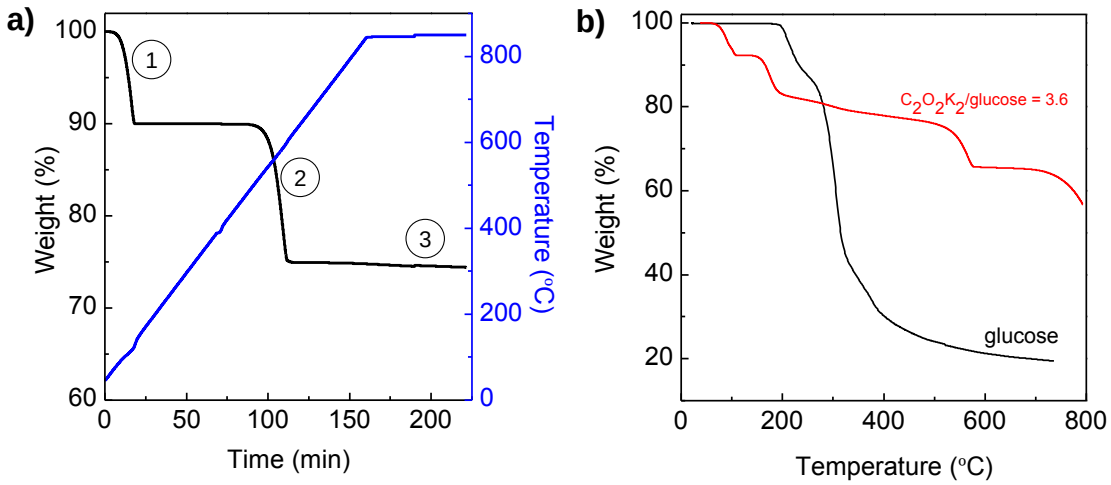

1. $C_2O_2K_2.H_2O \rightarrow C_2O_2K_2 + H_2O$ (10 % weight loss)
2. $C_2O_2K_2 \rightarrow K_2CO_3 + CO$ (~ 15 % weight loss)
3. $K_2CO_3 \rightarrow K_2O + CO_2$ (~ 0.6 % weight loss)

Figure S3. Thermogravimetric analysis of a) potassium oxalate, and b) glucose and a 3.6/1 mixture of potassium oxalate and glucose (heating at 3-5 ºC min^{-1}, N_2 atmosphere).

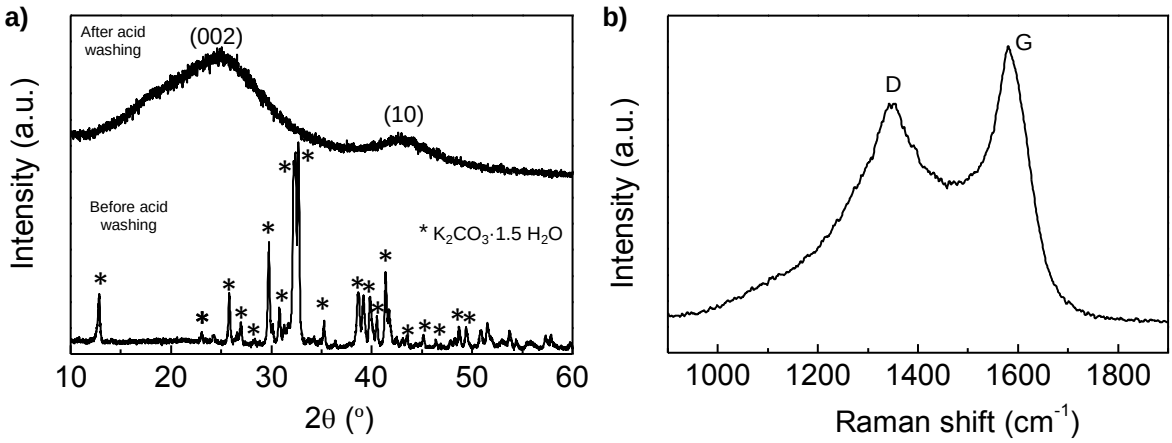

Figure S4. a) XRD patterns of G-800 before and after acid washing, and b) Raman spectrum of G-800.

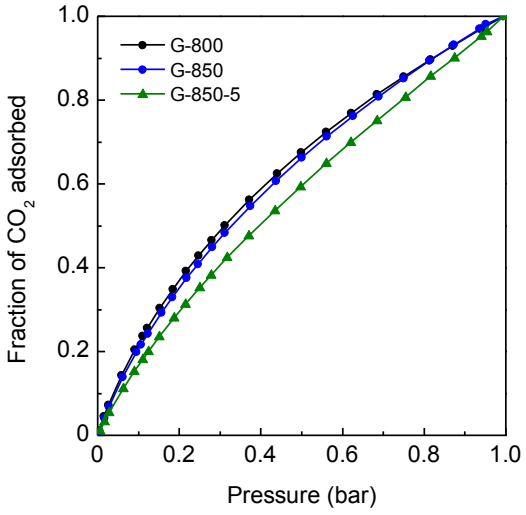

Figure S5. Fraction of CO_2 adsorbed as a function of pressure.

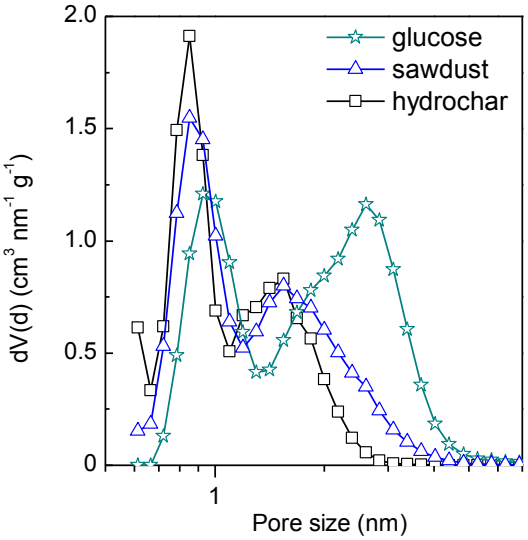

Figure S6. Pore size distributions of porous carbons obtained from hydrochar,[21] glucose and eucalyptus sawdust using a mixture of potassium oxalate and melamine as activating agent. Weight ratio of precursor/potassium oxalate/melamine = 1 / 3.6 / 2 and T = 800 ºC.

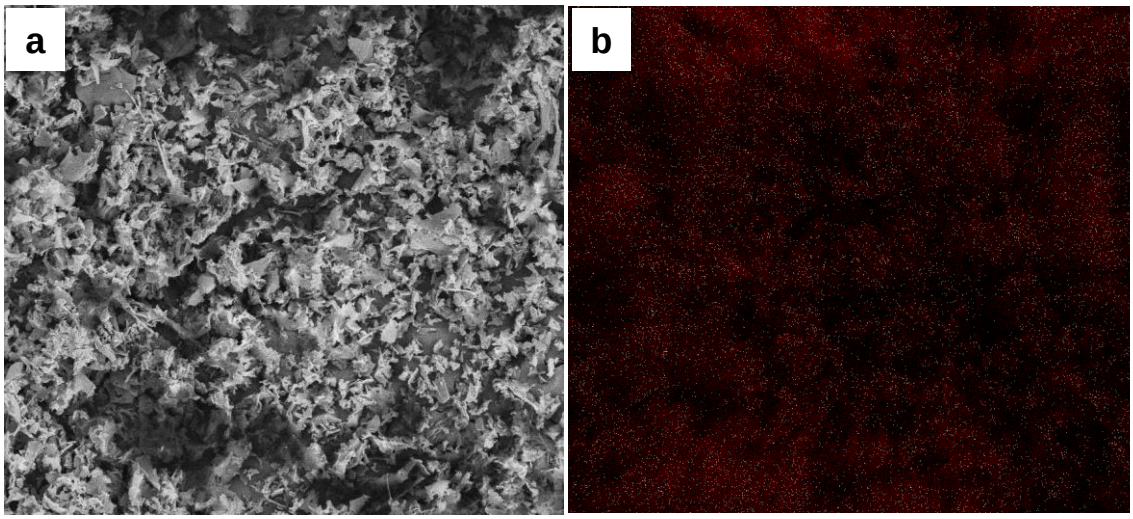

Figure S7. a) SEM image of sample G-3.6-2, and (b) the corresponding EDX mappings for carbon (red) and nitrogen (white).

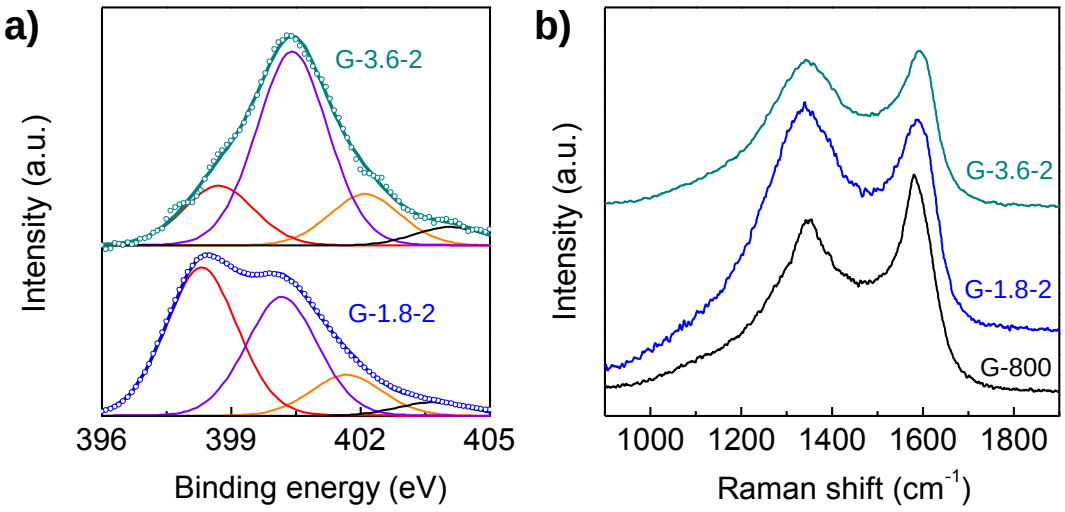

Figure S8. a) N 1s core level XPS spectra of the porous carbons G-1.8-2 and G-3.6-2, and b) first-order Raman spectra of G-800, G-1.8-2 and G-3.6-2.

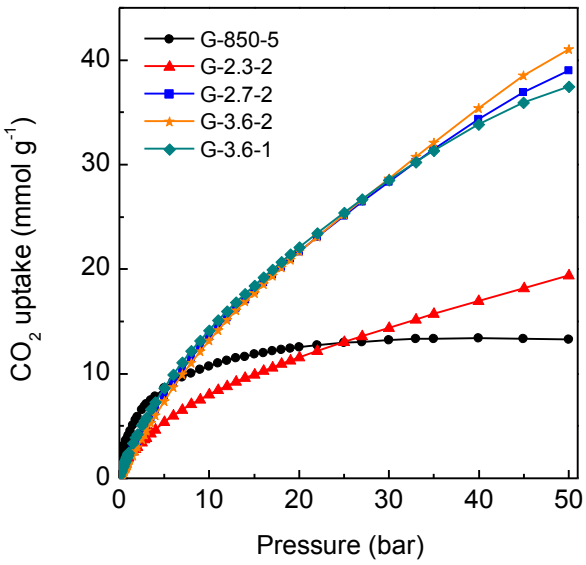

Figure S9. High-pressure excess CO_2 uptake isotherms at 25 ºC up to 50 bar for the microporous carbon G-850-5 and several micro-mesoporous carbons.

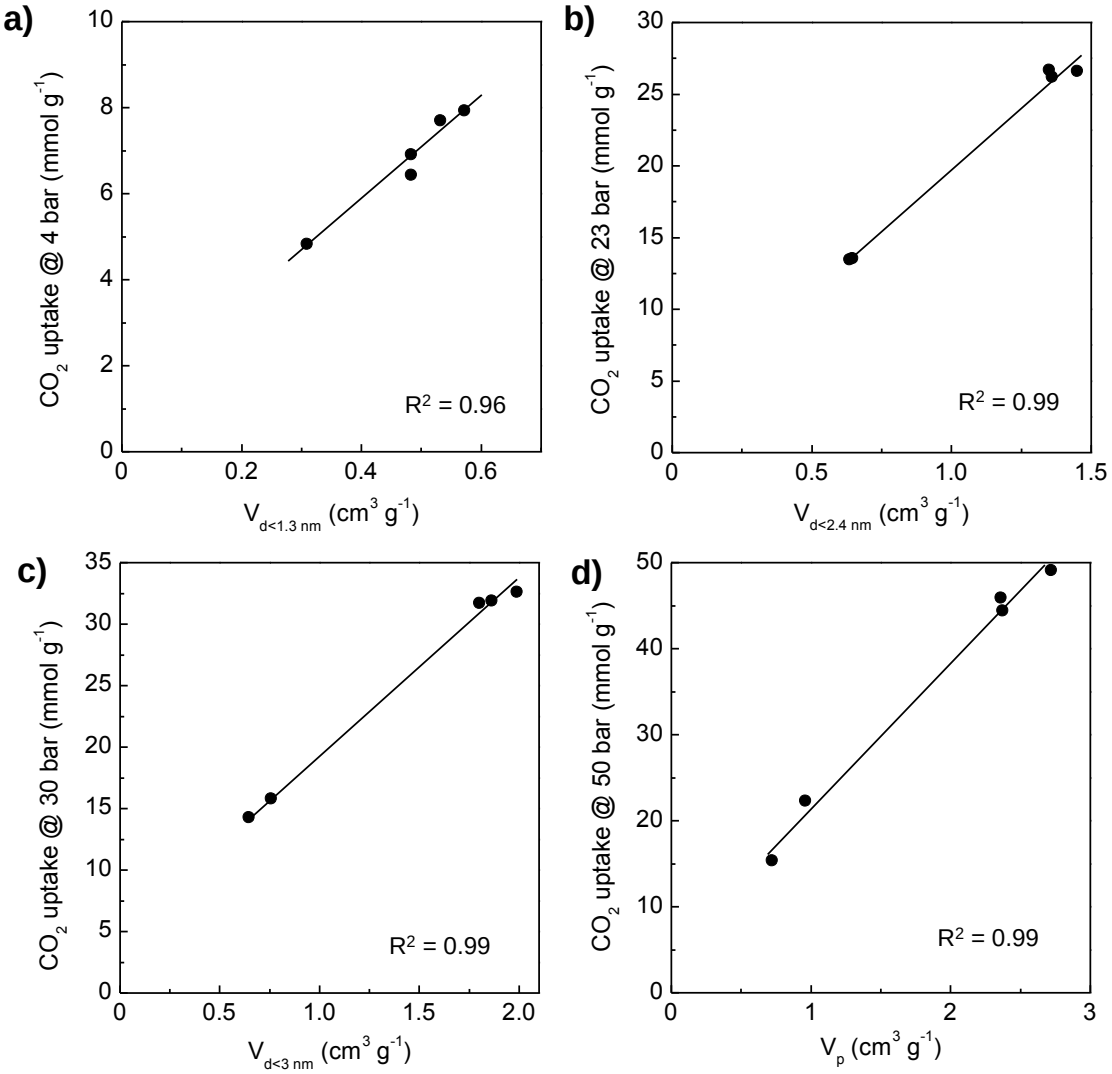

Figure S10. Correlation between the CO_2 uptake at 25 ºC and various pressures and the cumulative pore volume of pores below certain key size: a) 1.3 nm, b) 2.4 nm, c) 3 nm and d) total pore volume.

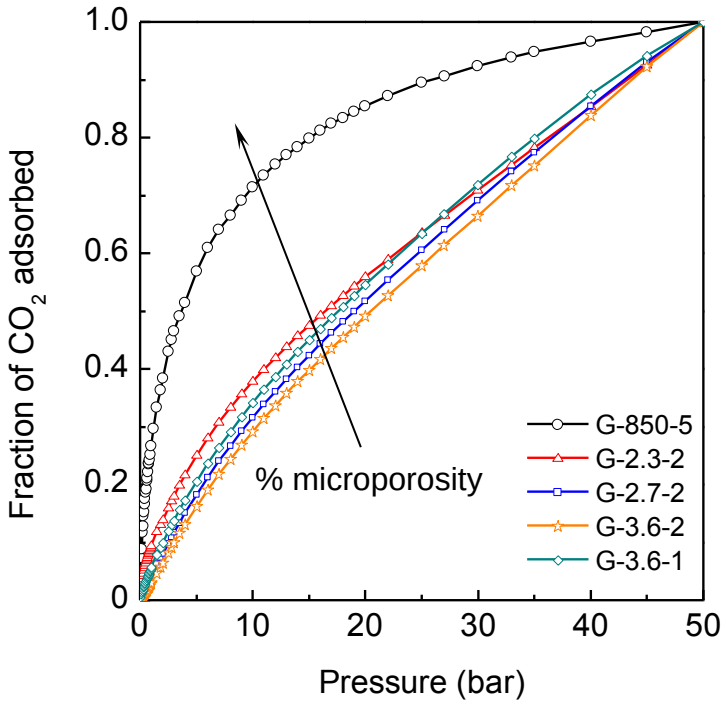

Figure S11. Fraction of CO_2 adsorbed as a function of pressure.

References:

[1] Wickramaratne, N. P.; Jaroniec, M. Activated Carbon Spheres for CO_2 Adsorption. *ACS App. Mater. Interfases* ***2013***, *5*, 1849-1855.

[2] Ludwinowicz, J.; Jaroniec, M. Potassium Salt-Assisted Synthesis of Highly Microporous Carbon Spheres for CO_2 Adsorption. *Carbon* ***2015***, *82*, 297-303.

[3] Sevilla, M.; Fuertes, A. B. Sustainable Porous Carbons with a Superior Performance for Co2 Capture. *Energy Environ. Sci.* ***2011***, *4*, 1765-1771.

[4] Zhou, J.; Li, Z.; Xing, W.; Zhu, T.; Shen, H.; Zhuo, S. N-Doped Microporous Carbons Derived from Direct Carbonization of K+ Exchanged Meta-Aminophenol-Formaldehyde Resin for Superior CO_2 Sorption. *Chem. Commun.* ***2015***, *51*, 4591-4594.

[5] To, J. W. F.; He, J.; Mei, J.; Haghpanah, R.; Chen, Z.; Kurosawa, T.; Chen, S.; Bae, W.-G.; Pan, L.; Tok, J. B. H.; Wilcox, J.; Bao, Z. Hierarchical N-Doped Carbon as CO_2 Adsorbent with High Co2 Selectivity from Rationally Designed Polypyrrole Precursor. *J. Am. Chem. Soc.* ***2016***, *138*, 1001-1009.

[6] Lee, D.; Zhang, C.; Wei, C.; Ashfeld, B. L.; Gao, H. Hierarchically Porous Materials Via Assembly of Nitrogen-Rich Polymer Nanoparticles for Efficient and Selective CO_2 Capture. *J. Mater. Chem. A* ***2013***, *1*, 14862-14867.

[7] Coromina, H. M.; Walsh, D. A.; Mokaya, R. Biomass-Derived Activated Carbon with Simultaneously Enhanced CO_2 Uptake for Both Pre and Post Combustion Capture Applications. *J. Mater. Chem. A* ***2016***, *4*, 280-289.

[8] Balahmar, N.; Mitchell, A. C.; Mokaya, R. Generalized Mechanochemical Synthesis of Biomass-Derived Sustainable Carbons for High Performance CO_2 Storage. *Adv. Energy Mater.* ***2015***, *5*, 1500867.

[9] Adeniran, B.; Mokaya, R. Compactivation: A Mechanochemical Approach to Carbons with Superior Porosity and Exceptional Performance for Hydrogen and CO_2 Storage. *Nano Energy* ***2015***, *16*, 173-185.

[10] Ashourirad, B.; Arab, P.; Islamoglu, T.; Cychosz, K. A.; Thommes, M.; El-Kaderi, H. M. A Cost-Effective Synthesis of Heteroatom-Doped Porous Carbons as Efficient Co2 Sorbents. *J. Mater. Chem. A* ***2016***, *4*, 14693-14702.

[11] Sethia, G.; Sayari, A. Comprehensive Study of Ultra-Microporous Nitrogen-Doped Activated Carbon for CO_2 Capture. *Carbon* ***2015***, *93*, 68-80.

[12] Ashourirad, B.; Sekizkardes, A. K.; Altarawneh, S.; El-Kaderi, H. M. Exceptional Gas Adsorption Properties by Nitrogen-Doped Porous Carbons Derived from Benzimidazole-Linked. Polymers. *Chem. Mater.* ***2015***, *27*, 1349-1358.

[13] Liu, L.; Xie, Z.-H.; Deng, Q.-F.; Hou, X.-X.; Yuan, Z.-Y. One-Pot Carbonization Enrichment of Nitrogen in Microporous Carbon Spheres for Efficient CO_2 Capture. *J. Mater. Chem. A* **2017**, *5*, 418-425.

[14] Sevilla, M.; Sangchoom, W.; Balahmar, N.; Fuertes, A. B.; Mokaya, R. Highly Porous Renewable Carbons for Enhanced Storage of Energy-Related Gases (H2 and CO_2) at High Pressures. *ACS Sustain. Chem. Eng.* ***2016***, *4*, 4710-4716.

[15] Casco, M. E.; Martínez-Escandell, M.; Silvestre-Albero, J.; Rodríguez-Reinoso, F. Effect of the Porous Structure in Carbon Materials for Co2 Capture at Atmospheric and High-Pressure. *Carbon* ***2014***, *67*, 230-235.

[16] Srinivas, G.; Krungleviciute, V.; Guo, Z.-X.; Yildirim, T. Exceptional CO_2 Capture in a Hierarchically Porous Carbon with Simultaneous High Surface Area and Pore Volume. *Energy Environ. Sci.* ***2014***, *7*, 335-342.

[17] Li, Y.; Ben, T.; Zhang, B.; Fu, Y.; Qiu, S. Ultrahigh Gas Storage Both at Low and High Pressures in KOH-Activated Carbonized Porous Aromatic Frameworks. *Sci. Rep.* ***2013***, *3*, 2420.

[18] He, J.; To, J. W. F.; Psarras, P. C.; Yan, H.; Atkinson, T.; Holmes, R. T.; Nordlund, D.; Bao, Z.; Wilcox, J. Tunable Polyaniline-Based Porous Carbon with Ultrahigh Surface Area for CO_2 Capture at Elevated Pressure. *Adv. Energy Mater.* ***2016***, *6*, 1502491.
[19] Jalilov, A. S.; Li, Y.;Tian, J.; Tour, J. M. Ultra-High Surface Area Activated Porous Asphalt for CO_2 Capture through Competitive Adsorption at High Pressures. *Adv. Energy Mater.* ***2017***, *7*, 1600693.
[20] Cox, M.; Mokaya, R. Ultra-High Surface Area Mesoporous Carbons for Colossal Pre Combustion CO_2 Capture and Storage as Materials for Hydrogen Purification. *Sustain. Energy Fuels* ***2017,*** *1,* 1414–1424.
[21] Sevilla, M.; Ferrero, G. A.; Fuertes, A. B. Beyond KOH Activation for the Synthesis of Superactivated Carbons from Hydrochar. *Carbon* ***2017***, *114*, 50-58.